An alcohol-sensing site in the calcium- and voltage-gated, large conductance potassium (BK) channel

Anna N. Bukiya, Guruprasad Kuntamallappanavar, Justin Edwards, Aditya K. Singh, Bangalore Shivakumar, and Alex M. Dopico[1]

Department of Pharmacology, College of Medicine, The University of Tennessee Health Science Center, Memphis, TN 38163

Edited by Richard W. Aldrich, The University of Texas at Austin, Austin, TX, and approved May 12, 2014 (received for review September 13, 2013)

Ethanol alters BK (slo1) channel function leading to perturbation of physiology and behavior. Site(s) and mechanism(s) of ethanol–BK channel interaction are unknown. We demonstrate that ethanol docks onto a water-accessible site that is strategically positioned between the slo1 calcium-sensors and gate. Ethanol only accesses this site in presence of calcium, the BK channel's physiological agonist. Within the site, ethanol hydrogen-bonds with K361. Moreover, substitutions that hamper hydrogen bond formation or prevent ethanol from accessing K361 abolish alcohol action without altering basal channel function. Alcohol interacting site dimensions are approximately 10.7 × 8.6 × 7.1 Å, accommodating effective (ethanol-heptanol) but not ineffective (octanol, nonanol) channel activators. This study presents: (*i*) to our knowledge, the first identification and characterization of an n-alkanol recognition site in a member of the voltage-gated TM6 channel superfamily; (*ii*) structural insights on ethanol allosteric interactions with ligand-gated ion channels; and (*iii*) a first step for designing agents that antagonize BK channel-mediated alcohol actions without perturbing basal channel function.

ethanol site | potassium channel | MaxiK channel | calcium sensitivity | patch-clamp electrophysiology

Alcohol (ethyl alcohol, ethanol) is a psychoactive agent that has been overwhelmingly consumed by mankind across cultures and civilizations. Alcohol actions on central nervous system (CNS) physiology and behavior are largely independent of beverage type but due to ethanol itself (1). Ethanol alters cell excitability by modifying function of transmembrane (TM) ion channel proteins, including K^+ channels. These channels constitute the most heterogeneous and extensive group of ion channels, its members belonging to TM2, TM4, and TM6 protein superfamilies. Within this myriad of proteins, several K^+ channels have been shown to modify behavior in response to acute exposure to ethanol concentrations that reach the CNS and other excitable tissues during alcohol drinking (2–5). However, with the sole exception of the TM2, G protein-regulated inward rectifier K^+ (GIRK) channel (6), there is no structural information on ethanol-K^+ channel protein interacting sites currently available.

Voltage/Ca^{2+}-gated, large conductance K^+ channels (BK), which are members of the TM6 voltage-gated ion channel superfamily, constitute major mediators of alcohol actions in excitable tissues. Acute exposure to ethanol levels reached in CNS during alcohol intoxication alters BK-mediated currents and thus, elicits widespread and profound modifications in physiology and behavior. In rodent models, acute ethanol exposure leads to reduced vasopressin, oxytocin and growth hormone release with consequent perturbation in physiology and behavior (7), altered firing rates in nucleus accumbens (8) and dorsal root ganglia neurons (9), and alcohol-induced cerebral artery constriction (10, 11). Moreover, studies in both mammals and invertebrate models demonstrate that ethanol targeting of neuronal BK is involved in development of alcohol tolerance and dependence (12–16). Although the physiological and behavioral consequences of ethanol disruption of BK function have been well documented, it remains unknown whether alcohol modification of BK function results from drug interaction with a defined recognition site(s) in a protein target vs. physical perturbation of the proteolipid environment where the BK protein resides. Thus, location and structural characteristics of the ethanol-recognition site(s), as well as nature of chemical bonds between ethanol and functional target that lead to modification of BK function, remain unknown.

Ethanol-induced regulation of BK channels is fine-tuned by many factors, including the BK channel-forming slo1 protein (α subunit) isoform (17) and its modification by phosphorylation (18), BK channel accessory (β) subunits (11), the channel-activating ionic ligand (Ca_i^{2+}) (19) and the lipid microenvironment around the BK protein complex (20). However, ethanol perturbation of BK function is sustained when the slo1 protein is probed with the alcohol in cell-free membrane patches (19–21) or after protein reconstitution into artificial lipid bilayers (22). We recently demonstrated that perturbation of slo1 function by ethanol concentrations reached in blood during alcohol intoxication does not extend to Na^+-gated slo2 and pH-gated slo3 channels, which are phylogenetically and structurally related to slo1. However, ethanol sensitivity does extend to a prokaryotic K^+ channel from *Methanobacterium thermoautotrophicum* (MthK) (23), a TM2 ion channel that shares basic Ca_i^{2+}-driven gating mechanisms with slo1 (24). Collectively, these studies lead us to hypothesize that ethanol-recognition site(s) involved in alcohol modification of BK current exists in the slo1 cytosolic Ca_i^{2+}-sensing tail domain (CTD).

Based on crystallographic data of the slo1 CTD and primary alignment of slo1-related ion channels that share ethanol sensitivity, we first identified eight putative ethanol recognition regions in the slo1 CTD. Using computational modeling, point amino acid substitutions and electrophysiology, we identified a distinct pocket as the ethanol-recognition site that leads to alcohol modification

Significance

Alcohol (ethanol) is one of the most widely consumed psychoactive agents. Ethanol's targets in the body include voltage/calcium-gated, large conductance potassium (BK) channels. Here we identified and characterized for the first time an alcohol-sensing site in BK channel-forming proteins. Our discovery opens new ground for rational design of tools to counteract the effects of ethanol intoxication that are mediated by BK channels. We anticipate that genetic or epigenetic modifications of the BK channel ethanol-recognition site could explain differential sensitivity to ethanol. Finally, since individuals with low sensitivity to ethanol are prone to developing heavy drinking habits, genetic, epigenetic or other mechanisms acting at the newly identified BK channel ethanol-recognition site might be considered as potential predictors for developing alcohol preference.

Author contributions: A.N.B. and A.M.D. designed research; A.N.B., G.K., and J.E. performed research; A.K.S. and B.S. contributed new reagents/analytic tools; A.N.B., G.K., J.E., and A.M.D. analyzed data; A.N.B. and A.M.D. wrote the paper.

The authors declare no conflict of interest.

This article is a PNAS Direct Submission.

[1]To whom correspondence should be addressed. E-mail: adopico@uthsc.edu.

This article contains supporting information online at www.pnas.org/lookup/suppl/doi:10.1073/pnas.1317363111/-/DCSupplemental.

of BK current. This site has a few common characteristics of alcohol-binding protein sequences (25), yet presents features that differ from those of the alcohol site described in GIRK (6). In opposition to GIRK currents, which can be potentiated by alcohol in absence of G proteins (6), ethanol modulation of BK currents is dependent on the presence of Ca_i^{2+} (19). Our data strongly suggest that ethanol access to the newly identified BK ethanol-recognition site depends on the Ca_i^{2+} levels associated with the slo1 CTD. Thus, current data not only provide a structural basis for understanding Ca_i^{2+}–alcohol allosterism on BK channels but could render structural insights on other ligand-gated channels that are activated by ethanol in presence of their natural ligand (26–30). Finally, present data document that the newly identified site plays a critical role in BK channel sensitivity to long-chain alkanols and explain the reported chain length differential sensitivity ("cutoff") of linear n-alkanols to modify BK current (31).

Identification of a distinct alcohol-sensing site in BK channels opens the door for rational design of pharmaceuticals to counteract widespread effects of alcohol intoxication in the body without altering basal BK channel function. Because this site is present in human BK protein (AAA92290.1), it is possible that genetic, epigenetic or other modifications of the alcohol-sensing site in BK channels could contribute to differential sensitivity to alcohol intoxication in humans. In addition, considering that individuals with low alcohol sensitivity are prone to developing heavy drinking (32), an altered profile of alcohol-sensing site on BK channels might be included as a potential predictor, along with other targets, for developing alcohol preference.

Results

Identification of Discrete Ethanol-Sensing Regions Within the BK Cytosolic Tail Domain. We have recently established that a CTD containing two Ca_i^{2+}-sensing, regulator of conductance for K^+ (RCK) domain(s) seems to be necessary to bestow voltage-gated K^+ (K_V) structures, whether having two (MthK) or six (mslo1, mouse brain slo1) TM segments, with sensitivity to intoxicating levels of ethanol (23). Primary alignment of CTDs from MthK (residues 117–336) and mslo1 (residues 344–1209) revealed eight regions with sequence similarity (Fig. 1*A*). Because mslo1 channels and their human homolog hslo1 are identically modulated by ethanol (19, 22) and require activating Ca_i^{2+} for such modulation (19), we used the recently available crystallographic structure of the hslo1 CTD (33) as a template to create a homology model of the mslo1 CTD in presence of Ca^{2+}. Following amino acid sequence alignment of mslo1 and MthK (protein A# O27564), we mapped eight regions in the CTD that shared amino acid similarity in mslo1 and MthK, and could contain ethanol-sensing site(s) (Fig. 1*A*). Thus, computational multifragment search was used to identify the energetically favorable positions of ethanol molecules on the putative alcohol-sensing regions (Fig. S1). To identify the regions that have the highest likelihood of accommodating ethanol molecules, we applied general criteria previously proposed for alcohol-recognition sites common to water-soluble and membrane-bound proteins: (*i*) alcohol binding sites are located near an α-helix (preferentially at the helix N terminus), (*ii*) alcohols form hydrogen bonds with amino acids within the site, and (*iii*) there is net positive charge in the vicinity of the site, which seems to favor alcohol–protein interaction (25). Region 2 (residues 354–367) was the only that satisfied the aforementioned criteria (Table 1). Indeed, the ethanol molecule is positioned at the N-terminal end of the S355–F363 α-helix with K361 acting as hydrogen donor to the oxygen atom of the primary alcohol, and R514 providing a net positive charge in the vicinity of the ethanol-sensing site (Fig. 1*B*, *Inset*).

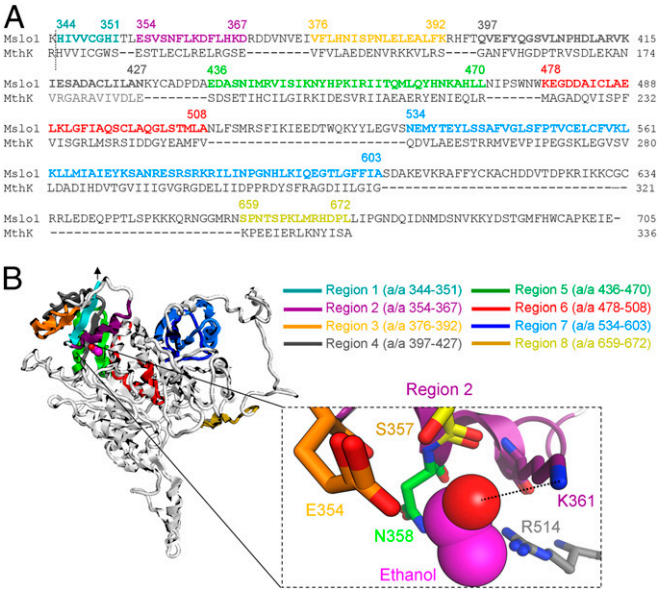

Fig. 1. Ethanol-sensing site in mslo1 CTD. (*A*) Sequence alignment of ethanol-sensitive mslo1 and MthK proteins reveals eight common regions that may provide ethanol-sensitivity. A dotted line indicates the *N*-end of the slo1 CTD based on crystallography (33). Amino acid numbering follows the numbering of corresponding hslo1 residues (33). (*B*) Putative ethanol-sensing regions mapped on the mslo1 CTD homology model (side view). The ethanol C chain is shown in pink; oxygen is in red. An arrow points at the *N*-end of the CTD in contact with the membrane. (*Inset*) The ethanol-sensing region 2 (a/a 354–367) where K361 hydrogen bonds (dotted line) with ethanol. Nitrogen is blue; hydrogen is hidden to improve display.

Table 1. Characterization of the computationally proposed alcohol-sensing sites

Site number	Limited groove, secluded "pocket"	Hydrogen bonding with alcohol	α-helix structure
1	No	Yes	No
2	**Yes**	**Yes**	**Yes**
3	Yes	Yes	No
4	Yes	Yes	No
5	No	Yes	Yes
6	No	No	No
7	No	Yes	No
8	No	No	No

Site 2 (boldfaced) is the only identified site that satisfies the criteria proposed for alcohol-sensing sites in proteins.

Substitutions of Critical Residues Within the Identified Ethanol-Docking Site Blunt BK Channel Sensitivity to Ethanol. To validate our computational predictions, we attempted to diminish the possibility of ethanol-K361 hydrogen bond formation and reduce net positive charge in the area by creating the double-mutant mslo1-K361N, R514N. Following in vitro transcription, the corresponding protein construct was expressed in *Xenopus* oocytes for patch-clamp experiments to test the ethanol sensitivity of the resulting ionic current, using WT mslo1 as a positive control. We chose inside-out (I/O) membrane patches with Ca_i^{2+} in solution tightly buffered at 0.3 μM, as this Ca_i^{2+} is physiological in most excitable cells and falls within a range that is optimal to evoke BK channel activation by intoxicating levels of ethanol (18–100 mM) (11, 19). After excision, each patch was exposed to control bath solution followed by application of 100 mM ethanol, which is ethanol E_{max} for modulating native BK and recombinant slo1 channel activity (21, 34). As consistently reported by us and others (11, 23, 35) when recording BK currents at sub-μM to low μM Ca_i^{2+}, 100 mM ethanol caused a ≥twofold reversible increase in

mslo1 steady-state activity (NPo) (Fig. 2 *A* and *C*). In contrast, mslo1-K361N, R514N channels were resistant to 100 mM ethanol (Fig. 2 *B* and *C*). This refractoriness cannot be explained by differences in basal (pre-ethanol) NPo between mutant and WT mslo1 (Fig. S2).

Ethanol sensitivity of slo and related proteins seems restricted to ion channels that are Ca_i^{2+}-gated (23). Therefore, we next evaluated whether the ethanol-resistance of the double mutant was selective for ethanol or, rather, accompanied by perturbation of gating by physiological changes in Ca_i^{2+} that activate WT slo1 channels (36–38). As expected, switching bath solution from 0.3 to 100 μM Ca_i^{2+} drastically increased mslo1 NPo and introduced a leftward shift in the macroscopic conductance (G)/G_{max} – voltage (V) relationship (Fig. 2*D* and Fig. S3 *A*, *B*, and *E*). In sharp contrast, this perturbation failed to modify mslo1-K361N, R514N NPo and $G/G_{max} - V$ plot (Fig. 2*D* and Fig. S3). In the context of previous data documenting that mutations that disrupted Ca_i^{2+}-sensing by the CTD RCK1 high-affinity site and the "Ca^{2+} bowl" also blunted ethanol action (19), and the fact that Ca_i^{2+}-sensing CTDs seem necessary for ethanol sensitivity of slo and related channels (23), the ethanol-resistance of mslo1-K361N,R514N currents may reflect: (*i*) alteration of structural elements responsible for specific ethanol–protein docking and/or (*ii*) generalized alteration of structures linked to Ca_i^{2+}-sensing. These hypotheses were tested by determining the alcohol sensitivity of mslo1 channels containing amino acid substitutions within the ethanol site.

As found for mslo1-K361N,R514N channels: (*i*) application of 100 mM ethanol to mslo1-R514N constructs consistently failed to increase NPo (Fig. 2 *C* and *E*), and (*ii*) switching bath solution from 0.3 to 100 μM Ca_i^{2+} did not evoke significant either an increase in NPo or $G/G_{max} - V$ plot leftward shift as observed in WT mslo1 (Fig. 2*D* and Fig. S3). These data implicate R514 as a key residue that functionally links slo1 Ca_i^{2+}-gating to ethanol sensing (*Discussion*). As found with mslo1-R514N, mslo1-K361N NPo failed to respond to 100 mM ethanol (Fig. 2 *C* and *F*). This result highlights the key role of K361 as hydrogen bond donor in ethanol-recognition by the slo1 CTD and eventual increase in NPo. However, mslo1-K361N showed voltage- and Ca_i^{2+}-sensitivities identical to those of WT mslo1 (Fig. S4), underscoring the role of K361 as a slo1 docking residue rather selective for the ligand ethanol.

Pocket isolation and creation of the ethanol receptor surface map show that R393 and K343 are located nearby, yet outside the proposed ethanol pocket (Fig. 3*A*). Thus, we introduced the R393N and K343N single substitutions to mslo1. The resulting mslo1-R393N and mslo1-K343N ion channels rendered $G/G_{max} - V$ plots and responses to 100 mM ethanol identical to those of WT mslo1 (Fig. 3 *B*–*E*), further validating our model where K361 and R514 are distinctively important in ethanol sensing as part of a discrete ethanol-sensing pocket where the ligand is bound to the BK channel protein.

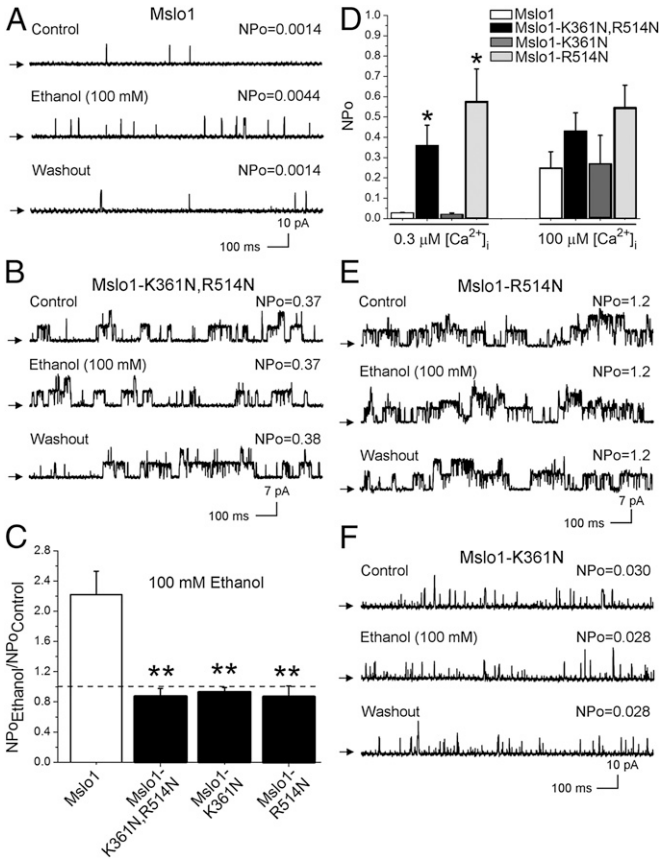

Fig. 2. Substitutions at K361 and R514 abolish ethanol action. (*A*) Reversible increase in WT mslo1 NPo with 100 mM ethanol. Ca_i^{2+} = 0.3 mM; unless stated otherwise, *Vm* = 60 mV. Arrows show the baseline (channels closed). (*B*) Lack of ethanol effect on mslo1-K361N,R514N; *Vm* = 30 mV. (*C*) Ethanol responses of mslo1 (n = 10) vs. mslo1-K361N,R514N (n = 10), mslo1-K361N (n = 15), and mslo1-R514N (n = 7). In all bar graphs, a dashed line indicates the point at which NPo is unchanged by ethanol; $^{**}P < 0.01$ vs. WT mslo1. (*D*) Ca_i^{2+} responses from mslo1-K361N,R514N, mslo1-R514N NPo *vs.* WT mslo1 ($^{*}P < 0.05$). Records from mslo1-R514N (*E*) and mslo1-K361N (*F*) show lack of ethanol effect; *Vm* = 30 mV and 60 mV, respectively.

Structural Bases of Ethanol Access to K361 and R514; Role of Ca_i^{2+}. Although both K361 and R514 are critical for ethanol functional recognition by slo1, R514 seems to be also involved in Ca^{2+}-sensing (Fig. 2*D* and Fig. S3). In addition, it has been reported that ethanol fails to modulate BK channel activity in the absence of Ca_i^{2+} (19). To provide the structural basis of these findings, we built an mslo1 CTD homology model based on the crystallographic structure of the hslo1 protein in its closed state, where Ca^{2+} is negligible (either absent or in contaminant trace below the levels required to activate the channel) (39). Computational superposition of mslo1 CTD homology model in a "Ca_i^{2+}-free" state with its open (Ca_i^{2+}-bound) state revealed major alterations in the ethanol-docking site (Fig. 3*F*): K361 is now stacked against M909. This spatial reorientation prevents the ethanol molecule from accessing K361 for hydrogen bonding. In addition, R514 moves away from the ethanol site when activating Ca_i^{2+} is absent (Fig. 3*F*). The distancing of R514 will diminish any possible facilitating effect of net positive charge on ethanol–protein interaction (25). Therefore, in a "Ca_i^{2+}-free" state(s) of mslo1, ethanol-sensing site loses the two essential structural features for ethanol activation of BK channels. These data may explain the ethanol refractoriness of slo1 channels in absence of activating Ca^{2+} (19).

After showing by computational models that in the "Ca^{2+}-free" mslo1 CTD ethanol may not be able to access its site, we decided to challenge ethanol's access to its site by introducing bulky substituents and, thus, impose a steric constraint on ligand access to the vicinity of K361. According to our model, residues E354, S357, and N358 are located within just 3–4 Å from the ethanol molecule positioned within the site (Fig. 1*B*, *Inset*). Substitution of listed residues with residues of a longer chain and larger volume rendered mslo1-E354Y, mslo1-S357Y and mslo1-N358W channels, which were consistently resistant to 100 mM ethanol even in presence of activating Ca_i^{2+} (Fig. 4*A*), as predicted from our model. In contrast, equivalent substitutions of N372, E374, and S382, which are located outside the proposed ethanol-sensing site (Fig. 4*C*), resulted in constructs with sensitivity to 100 mM ethanol identical to that of WT mslo1 (Fig. 4*D*).

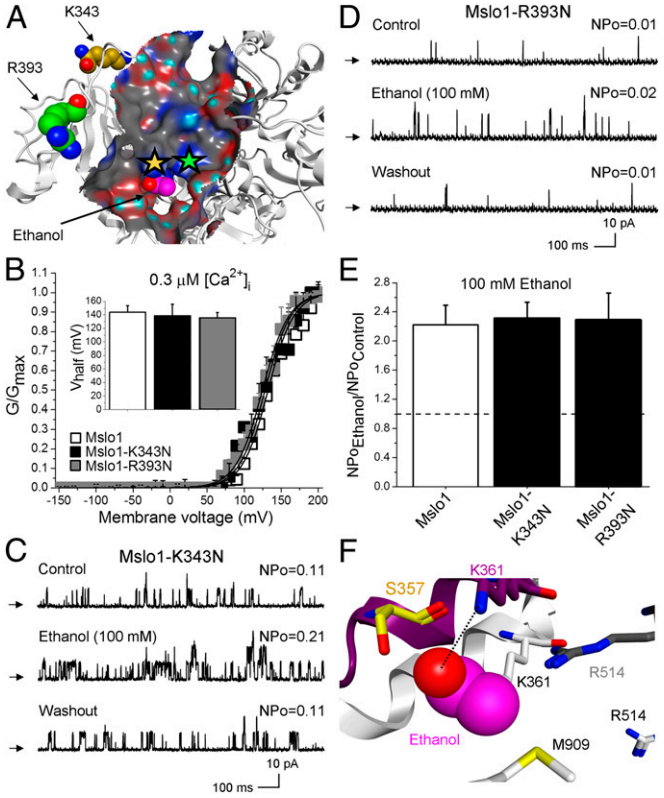

Fig. 3. K343 and R393 substitutions outside the alcohol-sensing site do not affect ethanol-induced mslo1 activation or the Ca_i^{2+} sensitivity of the channel. (*A*) Molecular surface map and location of K343 and R393. (*B*) $G/G_{max} - V$ plots from mslo1 ($n = 8$), mslo1-K343N ($n = 3$), and mslo1-R393N ($n = 3$) are undistinguishable. (*Inset*) V_{half} for the three constructs. Records from mslo1-K343N (*C*) and mslo1-R393N (*D*) show reversible increases in NPo by 100 mM ethanol. (*E*) WT mslo1 ($n = 10$), mslo1-K343N ($n = 8$), and mslo1-R393N ($n = 3$) NPo are increased by ethanol. (*F*) Superposition of the ethanol site in the "Ca^{2+}-bound" channel open state (color-coded as in Fig. 1*B*, *Inset*) with the "Ca^{2+}-free" channel closed state (black and white) of slo1.

As found for K361N, WT mslo1, mslo1-E354Y, mslo1-S357Y, and mslo1-N358W display identical Ca^{2+} sensitivity, which is evident from the similar leftward shift along the *V*-axis as Ca_i^{2+} is increased, and similar V_{half} values at each Ca_i^{2+} (Fig. 4*B* and Fig. S5). Thus, the loss of ethanol sensitivity in mslo1-E354Y, mslo1-S357Y, and mslo1-N358W experimentally validates the importance of ethanol access to K361 and underscores that refractoriness to ethanol in mutated mslo1 is not be necessarily linked to alteration in Ca^{2+}-sensing.

Ethanol-Recognition Site: Dimensions and its Role in slo1 Sensitivity to n-Alkanols. Slo1 activation by ethanol is dependent on the alcohol's chain length: n-alkanols display "cutoff" in activating BK currents, with ethanol, butanol, hexanol, and heptanol enhancing current, but octanol and nonanol having no effect (Fig. S6 and ref. 31). To experimentally determine the contribution of the newly identified ethanol pocket in n-alkanol action on slo1 channels, we probed mslo1-K361N channels with heptanol, the last (longest) in the series of n-alkanols that activate WT mslo1 (Fig. 5*A* and Fig. S6). Data show that 3 mM heptanol consistently failed to activate mslo1-K361N channels (Fig. 5 *B* and *C*), which highlights the role of this residue not only in ethanol but also in long-chain alkanol action on BK channels.

To provide a structural explanation for n-alkanol cutoff in BK channel activation, we created n-alkanol conformational libraries and used a docking routine to find representative poses for n-alkanol molecules within the newly identified ethanol-sensing site. Our results show that all n-alkanols that potentiate BK currents form hydrogen bonds with K361 and cluster in close vicinity to E354, S357, and N358 on the mslo1 CTD surface (Fig. 5*D*). Remarkably, although octanol and nonanol were still able to form hydrogen bonds with K361, both n-alkanols failed to fit in the immediate vicinity (3–4 Å) of E354, S357, and N358 (Fig. 5*D*). Thus, these computational data may explain the reported inability of octanol and nonanol to potentiate BK current (Fig. S6 and ref. 31). Moreover, "cutoff" of the alkanol chain length allows us to estimate dimensions of alkanol-sensing pocket: Cluster of n-alkanols that activate mslo1 fit the area of ~10.7 × 8.6 × 7.1 Å.

Discussion

Based on crystallographic structure, computational modeling, site-directed mutagenesis, and electrophysiology, we identified, to our knowledge for the first time, a discrete pocket for ethanol-docking and consequent channel activation in a member of the TM6 voltage-gated channel superfamily. The ethanol site resides in the CTD of the channel-forming subunit of the BK (slo1) channel. This location is in agreement with our earlier electrophysiological data suggesting that the slo1 CTD was the region that should contain ethanol-sensing site(s) (23). The intracellular topology of the BK channel alcohol-sensing site, however, is rather unusual for a transmembrane channel protein as ethanol-sensing motifs have been mapped to TM regions in many ligand-gated ion channels, such as mammalian GABA, glycine, nACh, and prokaryotic *Gloeobacter violaceus* (GLIC) channels (5, 40). A cytosolic location for an ethanol-docking site, however, is not exclusive to slo1 proteins: Intracellular alcohol-sensing pocket has been identified in the GIRK channel (6).

Dimensions of the cavity are also in general agreement with data obtained from alcohol-sensing pockets in eukaryotic GIRK and prokaryotic GLIC channels (6, 40). Indeed, as found in these

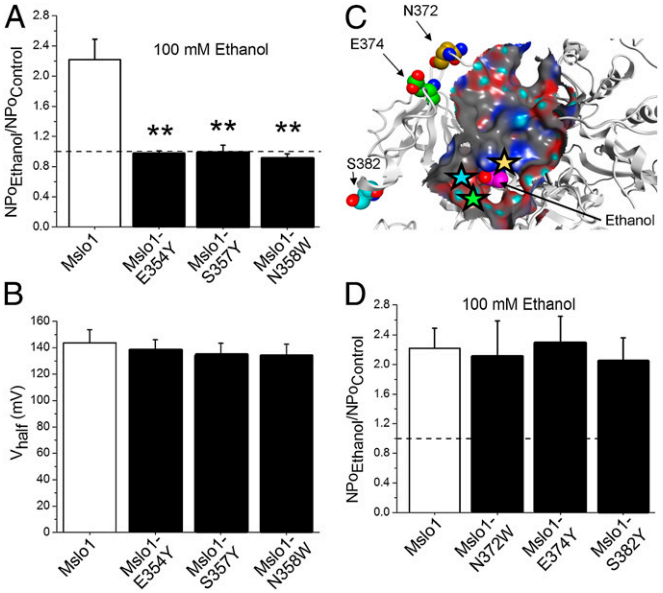

Fig. 4. Mutations that prevent ethanol from accessing K361 abolish ethanol-induced increase in mslo1 channel activity. (*A*) Ethanol responses of mslo1-E354Y ($n = 5$), mslo1-S357Y ($n = 3$), and mslo1-N358W NPo ($n = 4$) vs. WT mslo1; $^{**}P < 0.01$. (*B*) At $Ca_i^{2+} = 0.3$ mM, WT mslo1, mslo1-E354Y, mslo1-S357Y, and mslo1-N358W have similar V_{half}. (*C*) Molecular surface map highlights the location of N372, E374 and S382 outside the ethanol site. (*D*) Ethanol-induced increases in NPo are similar in mslo1 ($n = 10$), mslo1-N372W ($n = 5$), mslo1-E374Y ($n = 5$), and mslo1-S382Y ($n = 4$).

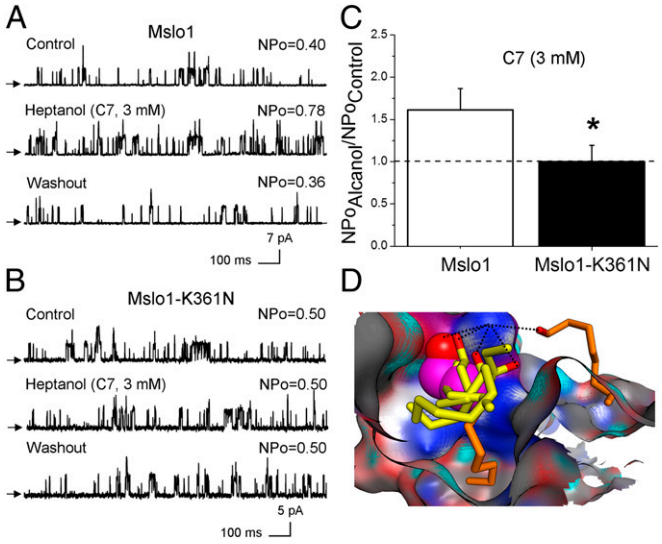

Fig. 5. Role of the ethanol site in long-chain alkanol effects on mslo1. Heptanol increases WT mslo1 (*A*) but not mslo1-K361N NPo (*B*). (*C*) Averaged responses to heptanol from mslo1 ($n = 4$) vs. mslo1-K361N NPo ($n = 3$). (*D*) Poses of n-alkanols on the ethanol site surface map. Ethanol C backbone is in pink; other activatory n-alkanols are shown in yellow, whereas ineffective n-alkanols are in orange. In all cases, oxygen is in red. Hydrogen bond is a dotted line.

channels, introduction of a bulky residue into the ethanol-sensing pocket of the BK channel (mslo1-E354Y, mslo1-S357Y, mslo1-N358W) abolishes ethanol action (Fig. 4*A*). In addition, n-alkanols that are powerful BK current activators fit within the proposed alcohol-sensing pocket on slo1, whereas n-alkanols unable to evoke BK current activation cannot locate within the alcohol-sensing pocket (Fig. 5*D*).

Hydrogen bonding between the alcohol molecule and protein seems to constitute a canonical interaction in alcohol-sensing protein sites (25, 40). Computational modeling based on crystallographic structure of the slo1 CTD shows appropriate distance and angle for hydrogen atoms of K361 side-chain to hydrogen-bond with the hydroxyl group of the n-alkanol (Fig. 1*B*, *Inset*). The key role of K361 residue is underscored by the fact that single conservative substitution K361 totally suppresses ethanol action, even when BK channel function was tested with 100 mM ethanol (Fig. 2 *A* and *C*), a concentration that represents E_{max} for activating recombinant and native BK channels (21, 34) and is usually lethal to naïve mammals including humans (41).

Despite the aforementioned general similarities, the BK channel ethanol-docking site does contain unique features: the occurrence of hydrogen bonding with a K residue differs from data from ligand-gated ion channels where alcohol hydrogen bonds not with K but other hydrophilic amino acid partners (E, N in GLIC; S, R, Q in α1 Gly, and S, N in nACh) (40). It has been proposed that presence of S or T residue represent characteristic motif of alcohol-sensing site, as these residues may form hydrogen bonds with n-alkanols (42). Thus, our data and work published by others (6, 40) reveal that n-alkanols do not have a unique hydrogen bond partner within alcohol-sensing sites.

Structural considerations reveal significant differences between the ethanol-sensing sites of BK and GIRK. For instance, polar residues within the GIRK alcohol-sensing pocket are aromatic (Y), whereas those in the BK site are aliphatic (E, S, N, or K; Fig. 1*B*, *Inset*). In addition, there are no amino acids carrying net positive charge within alcohol-sensing pocket on GIRK. In contrast, net positive charge presented by R514 is critical for ethanol-sensitivity of BK channel (Fig. 2 *C* and *E*). Finally, the ethanol-sensing site in BK channel is located in the vicinity of an α-helix (Fig. 1*B*), whereas the alcohol-sensing pocket in GIRK is defined by a β-sheet array (6).

The newly identified ethanol-sensing site on BK channel may explain the absolute dependence of ethanol modulation of BK channel function on Ca_i^{2+} levels (19, 23). After computational superposition of predicted ethanol-sensing site in presence vs. nominal zero Ca^{2+}, we demonstrate that K361 is not accessible for hydrogen bonding, and ethanol-sensing pocket is protruded by M909 (Fig. 3*F*) in the "Ca^{2+}-free" closed channel. Notably, K361 is adjacent to the RCK1 high-affinity Ca^{2+}-binding site determined by D362,D367 (33). In addition, R514 is neighbored by the M513, the amino acid that plays a key role in maintaining the structural integrity of Ca^{2+}-binding RCK1 domain in BK channels (39). Close spatial location of ethanol-sensing site and Ca_i^{2+}-sensing machinery raises the likelihood of cross-talking between these two ligands in modulating BK channel activity, this functional interaction being demonstrated by electrophysiological studies (19). Collectively, comparison of our BK channel structural data with those from GIRK, in connection with the fact that the presence of the channel's natural ligand is required for alcohol action in the former but not in the later, led us to speculate that the structural bases of natural ligand-alcohol allosterism found in BK channels could be a more applicable model for other naturally occurring ligand-gated ion channels, such as neuronal α4β2 nicotinic, homomeric α1 Gly, and GABA-A ionotropic receptors (26–30), which are potentiated by alcohol only in presence of their natural ligands.

Current data show that the individual K361N, E354Y, S357Y, and N358W substitutions abolish the channel ethanol-sensitivity, whereas the apparent Ca^{2+}-sensitivity remains unmodified (Fig. 4*B*). Therefore, ethanol sensitivity vs. Ca_i^{2+} sensitivity of BK channels involves different structural elements for ligand docking. Thus, Ca^{2+} and ethanol constitute heterotropic ligands of the BK ionotropic receptor. Moreover, although Ca_i^{2+} binding enables ethanol to modulate BK channel function, ethanol presence reduces the channel's response to its natural ion activator (19, 21). Substitutions in high-affinity Ca_i^{2+}-sensing sites in mslo1 suppress ethanol action (19), yet point substitutions in the ethanol-docking site do not alter Ca_i^{2+} gating (Fig. 4 *A* and *B*). Thus, we advance a model in which ethanol docking onto a rather specific BK channel discrete site and associated modulation of ionotropic receptor function depend on Ca^{2+} binding, as the ethanol-docking is strategically positioned between the high-affinity (physiological) Ca_i^{2+}-sensing sites and the channel gate. Interestingly, current data show that, although mslo1-K361N,R514N, mslo1-R514N, and mslo1-K361N all lack ethanol sensitivity, only the R514N-containing constructs display an altered Ca_i^{2+} sensitivity (Fig. 2 and Fig. S3). Notably, R514 is shifted away from the ethanol-sensing site when modeled in the "Ca^{2+}-free" state (Fig. 3*F*). Thus, R514 seems to be a key structural component in slo1 CTD that communicates ethanol- and Ca_i^{2+}-sensing machineries.

We previously demonstrated that CaM kinase II phosphorylation of T107 in the slo1 S0-S1 linker can override ethanol-induced potentiation of channel activity, even leading to channel inhibition in response to ethanol (18). Slo1 isoforms containing T107, however, are largely restricted to the bovine brain and aorta, whereas slo1 from the vast majority of tissues and species, including humans, contain nonphosphorylatable residues in position 107 or equivalent, this structural feature allowing channel activation by ethanol (18). Key residues that participate in ethanol-docking into our newly identified alcohol pocket, such as K361, are also highly conserved across mammalian species, including humans. Thus, it is possible to speculate that the varied and drastic modifications of physiology and behavior induced by ethanol activation of BK channels in most mammals (7–12, 15) are mediated by the site reported here, which requires future in vivo studies.

Materials and Methods

Computational Studies. Mslo1 (*Mus musculus* Ca_i^{2+}-activated K^+ channel α-1 subunit; protein A# Q08460.2) CTD structure was built using the homology modeling built-in suite of Molecular Operating Environment software (Chemical Computing Group). The crystal structure of the hslo1 protein CTD with either Ca^{2+}-bound [Protein Data Bank (PDB) ID 3MT5] or Ca^{2+}-free (PDB ID 3NAF) was used as template (33, 39). During protein homology modeling and multifragment search (see below) presence of specific ions was not considered. However, both procedures were performed with the dielectric constant of the exterior solvent set to 80 to mimic the CTD aqueous environment.

Amino acid sequence alignment of mslo1 and MthK (A#O27564) was performed in Molecular Operating Environment (MOE) to identify cytosolic regions in mslo1 protein that share sequence similarity with MthK and, thus, could include ethanol-sensing sites. Fifty ethanol molecules were randomly placed in the vicinity of each region in mslo1 CTD, probing one region at a time. Built-in multifragment search routine was run in MOE using MFF94 force field. Based on the lowest interaction potential energy (dU) between ethanol and each sensing region, the best position of ethanol was determined. Molecular surface for the ethanol-sensing pocket was created using automatic function in MOE. Surface covers receptor atoms within 4.5 Å of ethanol molecule. Docking of n-alkanols was performed using built-in suit in MOE. Representative poses depicting hydrogen bonding between alkanol molecule and K361 were chosen for display.

Mutagenesis, Electrophysiology, and Data Analysis. Mutagenesis, electrophysiology, and data analysis were performed as reported (11, 18) and described in *SI Materials and Methods*. Data are shown as mean ± SEM.

ACKNOWLEDGMENTS. We thank Maria Asuncion-Chin for technical assistance. This work was supported by National Institutes of Health Grant R37 AA11560 (to A.M.D.).

1. Fleming M, Mihic SJ, Harris RA (2001) *Ethanol*, eds Hardman JG, Limbird LE (McGraw-Hill, New York), pp 429–445. National Institute on Alcohol Abuse and Alcoholism (www.niaaa.nih.gov).
2. Dildy-Mayfield JE, Mihic SJ, Liu Y, Deitrich RA, Harris RA (1996) Actions of long chain alcohols on GABAA and glutamate receptors: Relation to in vivo effects. *Br J Pharmacol* 118(2):378–384.
3. Mihic SJ, et al. (1997) Sites of alcohol and volatile anaesthetic action on GABA(A) and glycine receptors. *Nature* 389(6649):385–389.
4. Mascia MP, Trudell JR, Harris RA (2000) Specific binding sites for alcohols and anesthetics on ligand-gated ion channels. *Proc Natl Acad Sci USA* 97(16):9305–9310.
5. Harris RA, Trudell JR, Mihic SJ (2008) Ethanol's molecular targets. *Sci Signal* 1(28):re7.
6. Aryal P, Dvir H, Choe S, Slesinger PA (2009) A discrete alcohol pocket involved in GIRK channel activation. *Nat Neurosci* 12(8):988–995.
7. Brodie MS, Scholz A, Weiger TM, Dopico AM (2007) Ethanol interactions with calcium-dependent potassium channels. *Alcohol Clin Exp Res* 31(10):1625–1632.
8. Martin G, et al. (2004) Somatic localization of a specific large-conductance calcium-activated potassium channel subtype controls compartmentalized ethanol sensitivity in the nucleus accumbens. *J Neurosci* 24(29):6563–6572.
9. Gruss M, et al. (2001) Ethanol reduces excitability in a subgroup of primary sensory neurons by activation of BK(Ca) channels. *Eur J Neurosci* 14(8):1246–1256.
10. Liu P, Xi Q, Ahmed A, Jaggar JH, Dopico AM (2004) Essential role for smooth muscle BK channels in alcohol-induced cerebrovascular constriction. *Proc Natl Acad Sci USA* 101(52):18217–18222.
11. Bukiya AN, Liu J, Dopico AM (2009) The BK channel accessory beta1 subunit determines alcohol-induced cerebrovascular constriction. *FEBS Lett* 583(17):2779–2784.
12. Treistman SN, Martin GE (2009) BK Channels: Mediators and models for alcohol tolerance. *Trends Neurosci* 32(12):629–637.
13. Ghezzi A, Pohl JB, Wang Y, Atkinson NS (2010) BK channels play a counter-adaptive role in drug tolerance and dependence. *Proc Natl Acad Sci USA* 107(37):16360–16365.
14. Ghezzi A, Atkinson NS (2011) Homeostatic control of neural activity: A Drosophila model for drug tolerance and dependence. *Int Rev Neurobiol* 99:23–50.
15. Bettinger JC, Leung K, Bolling MH, Goldsmith AD, Davies AG (2012) Lipid environment modulates the development of acute tolerance to ethanol in Caenorhabditis elegans. *PLoS ONE* 7(5):e35192.
16. Dillon J, et al. (2013) Distinct molecular targets including SLO-1 and gap junctions are engaged across a continuum of ethanol concentrations in Caenorhabditis elegans. *FASEB J* 27(10):4266–4278.
17. Liu P, Liu J, Huang W, Li MD, Dopico AM (2003) Distinct regions of the slo subunit determine differential BKCa channel responses to ethanol. *Alcohol Clin Exp Res* 27(10):1640–1644.
18. Liu J, Asuncion-Chin M, Liu P, Dopico AM (2006) CaM kinase II phosphorylation of slo Thr107 regulates activity and ethanol responses of BK channels. *Nat Neurosci* 9(1):41–49.
19. Liu J, Vaithianathan T, Manivannan K, Parrill A, Dopico AM (2008) Ethanol modulates BKCa channels by acting as an adjuvant of calcium. *Mol Pharmacol* 74(3):628–640.
20. Dopico AM, Bukiya AN, Singh AK (2012) Large conductance, calcium- and voltage-gated potassium (BK) channels: Regulation by cholesterol. *Pharmacol Ther* 135(2):133–150.
21. Dopico AM, Anantharam V, Treistman SN (1998) Ethanol increases the activity of Ca(++)-dependent K+ (mslo) channels: Functional interaction with cytosolic Ca++. *J Pharmacol Exp Ther* 284(1):258–268.
22. Crowley JJ, Treistman SN, Dopico AM (2003) Cholesterol antagonizes ethanol potentiation of human brain BKCa channels reconstituted into phospholipid bilayers. *Mol Pharmacol* 64(2):365–372.
23. Liu J, Bukiya AN, Kuntamallappanavar G, Singh AK, Dopico AM (2013) Distinct sensitivity of slo1 channel proteins to ethanol. *Mol Pharmacol* 83(1):235–244.
24. Pau VP, et al. (2011) Structure and function of multiple Ca2+-binding sites in a K+ channel regulator of K+ conductance (RCK) domain. *Proc Natl Acad Sci USA* 108(43):17684–17689.
25. Dwyer DS, Bradley RJ (2000) Chemical properties of alcohols and their protein binding sites. *Cell Mol Life Sci* 57(2):265–275.
26. Lovinger DM (1996) Interactions between ethanol and agents that act on the NMDA-type glutamate receptor. *Alcohol Clin Exp Res* 20(8, Suppl):187A–191A.
27. Harris RA (1999) Ethanol actions on multiple ion channels: Which are important? *Alcohol Clin Exp Res* 23(10):1563–1570.
28. Mihic SJ (1999) Acute effects of ethanol on GABAA and glycine receptor function. *Neurochem Int* 35(2):115–123.
29. Dopico AM, Lovinger DM (2009) Acute alcohol action and desensitization of ligand-gated ion channels. *Pharmacol Rev* 61(1):98–114.
30. Yevenes GE, Zeilhofer HU (2011) Allosteric modulation of glycine receptors. *Br J Pharmacol* 164(2):224–236.
31. Chu B, Treistman SN (1997) Modulation of two cloned potassium channels by 1-alkanols demonstrates different cutoffs. *Alcohol Clin Exp Res* 21(6):1103–1107.
32. Schuckit MA, et al. (2011) A prospective evaluation of how a low level of response to alcohol predicts later heavy drinking and alcohol problems. *Am J Drug Alcohol Abuse* 37(6):479–486.
33. Yuan P, Leonetti MD, Pico AR, Hsiung Y, MacKinnon R (2010) Structure of the human BK channel Ca2+-activation apparatus at 3.0 A resolution. *Science* 329(5988):182–186.
34. Dopico AM, Lemos JR, Treistman SN (1996) Ethanol increases the activity of large conductance, Ca(2+)-activated K+ channels in isolated neurohypophysial terminals. *Mol Pharmacol* 49(1):40–48.
35. Feinberg-Zadek PL, Treistman SN (2007) Beta-subunits are important modulators of the acute response to alcohol in human BK channels. *Alcohol Clin Exp Res* 31(5):737–744.
36. Cui J, Cox DH, Aldrich RW (1997) Intrinsic voltage dependence and Ca2+ regulation of mslo large conductance Ca-activated K+ channels. *J Gen Physiol* 109(5):647–673.
37. Vergara C, Latorre R, Marrion NV, Adelman JP (1998) Calcium-activated potassium channels. *Curr Opin Neurobiol* 8(3):321–329.
38. Salkoff L, Butler A, Ferreira G, Santi C, Wei A (2006) High-conductance potassium channels of the SLO family. *Nat Rev Neurosci* 7(12):921–931.
39. Wu Y, Yang Y, Ye S, Jiang Y (2010) Structure of the gating ring from the human large-conductance Ca(2+)-gated K(+) channel. *Nature* 466(7304):393–397.
40. Sauguet L, et al. (2013) Structural basis for potentiation by alcohols and anaesthetics in a ligand-gated ion channel. *Nat Commun* 4:1697.
41. Diamond I (1992) *Cecil Textbook of Medicine*, eds Wyngaarden JB, Smith LH, Plum F (Saunders, Philadelphia), pp 44–47.
42. Kruse SW, Zhao R, Smith DP, Jones DN (2003) Structure of a specific alcohol-binding site defined by the odorant binding protein LUSH from Drosophila melanogaster. *Nat Struct Biol* 10(9):694–700.